Publisher homepage: www.universepg.com, ISSN: 2663-7804 (Online) & 2663-7790 (Print)

https://doi.org/10.34104/ajeit.024.051069

Australian Journal of Engineering and Innovative Technology

Journal homepage: www.universepg.com/journal/ajeit

Geospatial Assessment of Urban Sprawl: A Case Study of Herat City, Afghanistan

Ahmad Shakib Sahak[1,2]*, Fevzi Karsli[1], Karimullah Ahmadi[3,4], Mohammad Anwar Saraj[5], and Ahmad Tamim Sahak[5]

[1]Dept. of Geomatics, Faculty of Engineering, Karadeniz Technical University, Trabzon, Turkey; [2]Dept. of Geographical Information System Kabul Polytechnic University, Kabul, Afghanistan; [3]Dept. of Aerospace Research of the Earth, Photogrammetry, Moscow State University of Geodesy and Cartography, Moscow, Russian Federation; [4]Dept. of Civil Engineering, Nangarhar University, Jalalabad, Afghanistan; and [5]Dept. of Engineering Geodesy, Faculty of Geomatics and Cadaster, Kabul Polytechnic University, Kabul, Afghanistan.

*Correspondence: sh.sahak@kpu.edu.af (Ahmad Shakib Sahak, Ph.D. Candidate, Dept. of Geomatics, Karadeniz Technical University, 401530, Trabzon, Turkey).

ABSTRACT

This study aims to investigate the spatial and temporal dynamics of urban sprawl in Herat City, Afghanistan, from 2000 to 2021 using GIS and remote sensing data (Landsat 7 and 8). In this study, three machine learning algorithms, namely Support Vector Machine (SVM), Random Forest (RF), and Classification and Regression Trees (CART), were employed to classify the study area, and the accuracy of each algorithm for each study period was assessed. Based on the assessment results, the RF algorithm demonstrated higher accuracy and was selected as the classification algorithm. The Google Earth Engine cloud platform was utilized to classify the study area, and the GIS environment was employed for the creation of thematic layers. The analysis revealed a 30.06% increase in built-up areas from 2000 to 2021. Conversely, vegetation, water bodies, and bare land decreased by 8.51%, 1.08%, and 20.53%, respectively, during the same period. The findings indicated that Herat City experienced high-speed expansion between 2000 and 2013, while from 2013 to 2021; it developed at a medium speed. The Relative Shannon's entropy statistical algorithm was employed to quantify urban sprawl, and the results suggest a dispersed urban sprawl pattern. Internal migration to major cities due to conflicts, limited employment opportunities, and inadequate living amenities in rural areas has been a primary driver of urban sprawl in Herat City, Afghanistan.

Keywords: Urban sprawl, RF, CART, Shannon's entropy, UEII, SVM, Geospatial, Afghanistan, and Herat city.

INTRODUCTION:

"Urban sprawl" refers to a type of spatial growth distinguished by its low population density, scattered and discontinuous expansion that skips over areas, and the separation of different land uses (Manesha *et al.,* 2021; Patra *et al.,* 2022a). The expansion of urban sprawl has a direct consequence on altering the land use and land cover (LULC) of the region by accelerating the growth of developed and impermeable areas (Antalyn & Weerasinghe, 2020; Sudhira & Ramachandra, 2007). This has raised significant concerns about

the potential ecological risks posed by urban encroachment to the fundamental pillars of rural livelihoods, including forests, agriculture, and related sectors (Antalyn & Weerasinghe, 2020; Sudhira & Ramachandra, 2007). It encompasses key attributes such as development with a singular purpose, fragmentation, irregular shapes, low concentration or inequality, and the linear expansion (Aguilera *et al.,* 2011; Antalyn and Weerasinghe, 2020; Keita *et al.,* 2021; Liu and Meng, 2020; Manesha *et al.,* 2021; Mosammam *et al.,* 2017; Sudhira and Ramachandra, 2007; Verbeek *et al.,* 2014; Wei and Ewing, 2018). Therefore, urban sprawl has played a significant role in transforming rural land use patterns into urban ones, reducing the availability of rural land (Manesha *et al.*, 2021; Nejadi *et al.*, 2011). When discussing sprawl, the opposite concept is compact urban development, and sprawl is primarily characterized by the worry of a city's expansion occurring in an unplanned and unregulated manner (Manesha *et al.*, 2021). Urban sprawl poses significant challenges that have a detrimental impact on the prospects of achieving sustainable urban development (Páez & Scott, 2004). Effective management of urban development plays a crucial role in ensuring sustain-able urban development (Aguilera *et al.*, 2011; Wei and Ewing, 2018). This information significantly benefits urban planners and other professionals in related fields, helping them comprehend suitable methods for evaluating urban sprawl (Milad *et al.*, 2017). At present, planners and policy maker's extensively employ contemporary methods like Geographic Information Systems (GIS) and Remote Sensing (RS) to characterize spatial phenomena (Liu & Meng, 2020). GIS and RS are employed to address the spatiotemporal aspect, enabling the monitoring, regulation, analysis, assessment, and the measurement of urban growth patterns and alterations in land use (Ramachandra *et al.*, 2013). As a result, various statistical scales and parameters have been created to gauge urban sprawl by integrating these GIS and RS methods (Páez & Scott, 2004). Among these options, the utilization of Shannon's entropy approach and the Urban Expansion Intensity Index stands out as potent quantitative methods for assessing urban growth (Alsharif *et al.*, 2016; Boori *et al.*, 2015; Manesha *et al.*, 2021; Milad *et al.*, 2017; Mosammam *et al.*, 2017; Patra *et al.*, 2022a; Sridhar *et al.*, 2020). These indices hold importance for various reasons, including their ability to determine the pace of urban expansion, assess urban development patterns, and evaluate and track urban phenomena over different time intervals (Ramachandra *et al.*, 2013; Alom MJ., 2024). Conversely, landscape metrics are employed to evaluate the spatiotemporal characteristics of urban sprawl, encompassing attributes like disorder, aggregation, intricacy, and the degree of dispersion among urban land classes within the landscape of the study area (Manesha *et al.*, 2021; Taubenböck *et al.*, 2009).

Over the past two decades in Afghanistan, urban expansion especially in major cities, has led to the emergence of densely populated slums and extensive settlements on the outskirts of cities. This rapid urbanization has resulted in cities consuming large tracts of land to accommodate new developments. In certain areas, the rate of urban growth has outpaced the growth of the urban population, leading to less concentrated, poorly organized and inefficient land-use arrangements. The urban population in Afghanistan is continuously growing, leading to uncontrolled and swift urban development (Kristy, 2018a). Projections indicate that Afghan cities are expected to experience a doubling of their population in the next 15 years (UN-Habitat, 2015). By 2060, it is estimated that one out of every Afghan will be living in urban areas (UN-Habitat, 2015). To manage this transformation effectively and harness it for economic and social progress, accurate data and information are crucial (UN-Habitat, 2015).

Referring to the 2015 report by (UN-Habitat, 2015), it is evident that Afghan cities hold significant importance in fostering social and economic development, state-building, and peace-building efforts. Nonetheless, their complete potential has been limited by the lack of appropriate urban regulations and policies, inadequate and disjointed investments, and insufficient municipal governance and land management (UN-Habitat, 2015). For this study, Herat City has been chosen as the designated research area. Herat stands out as one of the rapidly expanding urban centers in western Afghanistan (UN-Habitat, 2015). In 2021, the urban population of Herat City reached 636,000, indicating a growth rate of 4.95% compared to the previous year, 2020 (UN-Habitat, 2015). A clear

correlation exists between population size and the progress of urban development (Bhatta 2009; Patra *et al.*, 2022b). The combination of unregulated urban expansion and population growth has driven the process of urbanization in Herat City (UN-Habitat, 2015). Numerous investigations have been conducted in Herat city regarding the topic of urban development (Ali Mahaqi *et al.*, 2020; Kristy, 2018b).

The conducted studies predominantly concentrated on the ramifications of urban development on cultural heritage, and also, they examined various facets linked to the environmental hydro-geochemical attributes, controlling variables, and the assessment of groundwater quality within Herat City. As a result, a quantitative investigation of the urban sprawl utilizing Shannon's entropy approach and the Urban Expansion Intensity Index in Herat City is currently lacking. Upon reviewing the pertinent literature, it is evident that there has been no prior research conducted in Herat City, Afghanistan, that specifically addresses the measurement of urban growth using the Shannon's entropy approach and the Urban Expansion Intensity Index, and this study will mark the inaugural research endeavor in this geographical region. The research methodologies and microscale approach employed in this study will offer utility to quantify urban expansion using Shannon's entropy approach and the Urban Expansion Intensity Index in cities of varying sizes, including small, medium, and large urban areas. As a result, this research seeks to assess the rate of urban expansion and urban development in Herat City by employing Shannon's entropy approach and the Urban Expansion Intensity Index through the utilization of optical remote sensing data. The outputs of this research will serve as valuable tools for policymakers at the Ministry of Urban Development and Land of Afghanistan, the Herat Municipality, the National Environmental Protection Agency (NEPA) of Afghanistan, and various other domestic and the inter national organizations involved. They will help these stakeholders comprehend the trajectory of urban expansion and formulate appropriate strategies and the policies to promote sustainable development in Afghanistan's major cities.

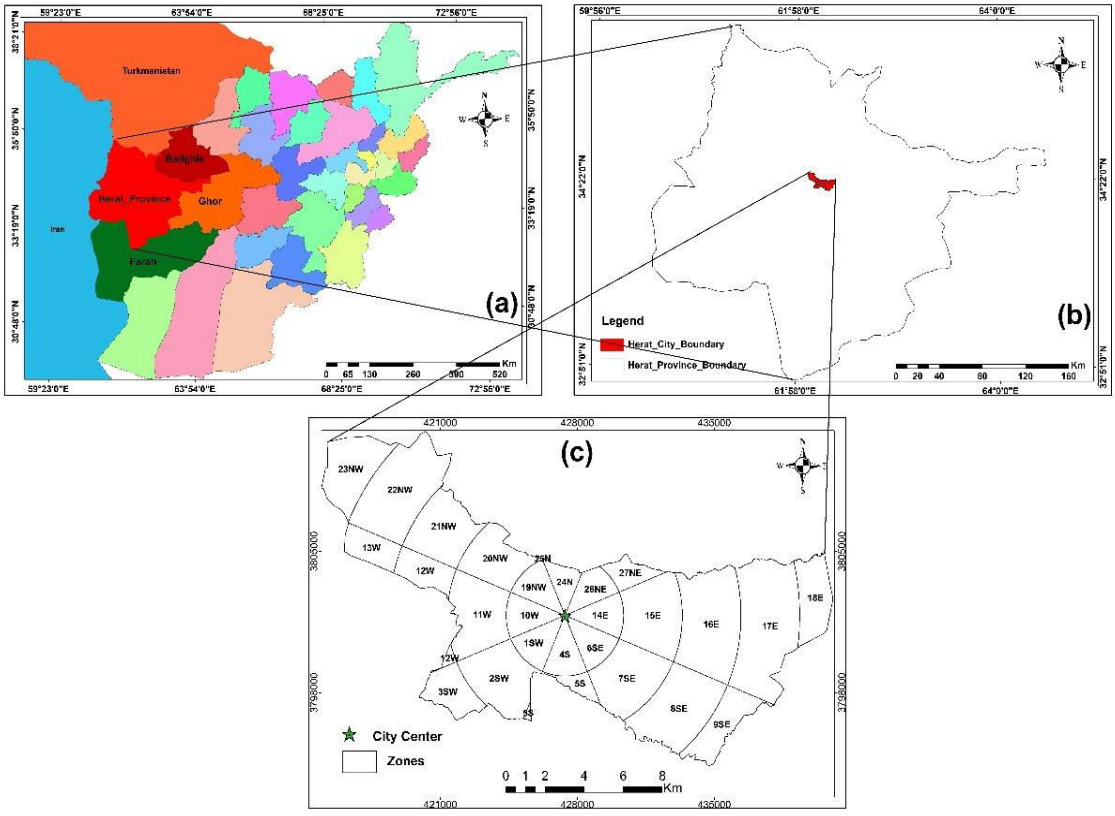

Fig. 1: The geographic location of the study area.

Study area

Herat province is located in the western part of Afghanistan, positioned at a latitude of 34°20′31″ North and a longitude of 62°12′11″ East (**Fig. 1**). To the east, it shares its border with Iran at the Islam Qala crossing, and to the north, it borders Turkmenistan at the Torghundi crossing. In Afghanistan, Herat province shares its boundaries with Badghis, Ghor, and Farah provinces (Nasery *et al.*, 2021a).

Herat city, situated in western Afghanistan, serves as the capital of the Herat province, and has gained recognition for its rapid development. Its history as a settlement trace back to ancient periods, including the Iron Age. Even in pre-Islamic epochs, especially during the reign of Alexander the Great, the city held a prominent and well-established position (Kristy, 2018b). In the past, Herat city faced destruction as a result of historical conflicts, including invasions by both Genghis Khan and Timur. However, during the reign of Sharooz, a leader from the Timurid dynasty, significant initiatives were launched to rebuild and develop the city, with a particular emphasis on expanding and beautifying it (Urban Development Threatens the Old City of Herat | UNAMA, n.d.). During July, Herat typically sees an average high temperature of 30°C, whereas in January, the minimum temperature decreases to 4°C (Nasery *et al.*, 2021b). Over the past 21 years, Herat city has witnessed a considerable influx of immigrants and rapid population growth. Unfortunately, this has resulted in significant degradation of the natural land cover, causing the once-pristine scenery and landscapes to disappear. Therefore, urban development has expanded rapidly within the city. To comprehensively assess the extent of urbanization, including impervious surfaces and other spatial characteristics, Herat city was chosen as the primary focal point for this research.

METHODOLOGY:

This study utilized multispectral data, namely Landsat 7 and Landsat 8 for the years 2000, 2013, and 2021 to create land use land cover within Herat city with higher accuracy (**Table 1**). In this study we employed the Cloud Computing Platform of Google Earth Engine (GEE), to classify the study area. The atmospherically corrected surface reflectance from the Landsat 7 and Landsat 8 dataset are used. This study utilized three machine learning algorithms: SVM, RF, and CART, to categorize the study area. The accuracy of each algorithm was evaluated for each study period.

Following the assessment, the RF algorithm classified the study area with higher accuracy and was chosen as the classification method. The study area was classified using the GEE cloud platform, and thematic layers were generated within the GIS environment. To identify and quantify urban patterns such as built-up areas as spatial phenomena, both the Urbanization Intensity Index and Shannon's entropy were computed. The following techniques are discussed below.

Table 1: Description of satellites Landsat 8 OLI/TIRS and Landsat 7.

Landsat 8 OLI/TIRS			**Landsat 7**		
Band NO	Wavelength (µm)	Pixel Size	Band NO	Wavelength (µm)	Pixel Size
B1	0.43-0.45	30 m	B1	0.45 – 0.52	30 m
B2	0.45-0.51	30 m	B2	0.52 – 0.60	30 m
B3	0.53-0.59	30 m	B3	0.63 – 0.69	30 m
B4	0.64-0.67	30 m	B4	0.77 – 0.90	30 m
B5	0.85-0.88	30 m	B5	1.55 – 1.75	30 m
B6	1.57-1.65	30 m	B6	10.40 12.50	60* (30 m)
B7	2.11-2.29	30 m	B7	2.09 – 2.35	30 m
B8	0.50-0.68	15 m	B8	0.52 – 0.90	15m
B9	1.36-1.38	30 m			
B10	10.6-11.19	100 m			
B11	11.50-12.51	100 m			

Quantification of urban sprawl

Urban Expansion Intensity Index

The Urban Expansion Intensity Index, abbreviated as UEII, can be employed to quantitatively assess the variations in urban spatial expansion. Furthermore, UEII can be utilized to identify urban growth patterns and to compare the rate or speed of changes in urban land use within a specific timeframe. Formula (1) illustrates the equation used for calculating UEII.

$$UEII_{it} = \left[\frac{ULA_{i,b} - ULA_{i,a}}{t}\right] / TLA_i \times 100 \quad (1)$$

In this equation, $UEII_{it}$ represents the annual average urban expansion intensity index for the (i_{th}) zone during time period (t). $ULA_{i,a}$ and $ULA_{i,b}$ denote the built-up area quantities at time periods a and b in the (i_{th}) spatial zone, respectively. TLA_i stands for the total area of the (i_{th}) spatial zone(Al-sharif *et al.*, 2016; Manesha *et al.*, 2021; Milad *et al.*, 2017). The UEII has been categorized into various groups, as depicted in **Table 2**.

Table 2: The division standard of Urban Expansion Intensity Index (UEII).

UEII	Speed
0 to 0.28	Slow
0.28 to 0.59	Low-Speed
0.59 to 1.05	Medium-Speed
1.05 to 1.92	High-Speed
Greater than 1.92	Very High-Speed

Shannon's Entropy Model

Shannon's entropy is a widely recognized approach for evaluating patterns of urban expansion (Antalyn & Weerasinghe, 2020; Bhatta *et al.*, 2010a; Manesha *et al.*, 2021). Shannon's entropy can be applied to gauge the level of spatial clustering or dispersion of a geographic variable (xi) across n zones (Yang, 2018). Shannon's urban entropy quantifies the degree of spatial density and dispersion of built-up land cover across various time intervals (Abubakr *et al.*, 2015; Rahman *et al.*, 2011; Verma *et al.*, 2017). The equation below is employed for computing Shannon's entropy (Jat *et al.*, 2008b):

$$H_n = \sum_i^n P_i Log_e\left(\frac{1}{P_i}\right) \quad (2)$$

To scale up the entropy values from 0 to 1, relative Shannon's entropy will be used. The following equation is used to estimate relative entropy (Thomas, 1981).

$$H'_n = \sum_i^n P_i Log_e\left(\frac{1}{P_i}\right) / Log_e(n) \quad (3)$$

$$P_i = \frac{X_i}{\sum_{i=1}^n X_i}$$

Where P_i stands for the probability or proportion of the variable (in this case, the built-up area) occurring in the ith zone, X_i represents the estimated value of the variable in the i_{th} zone, and n is the total number of zones. Shannon's entropy values fall within the range of 0 to log(n). When the value is closer to zero, it signifies concentrated urban growth, while a value closer to log(n) indicates a more dispersed pattern in the built-up environment (Yeh & Li, 2001). The rate of change in urban sprawl is computed using the following equation.

$$\Delta H_n = H_n(t_2) - H_n(t_1) \quad (4)$$

Where, $H_n(t_1)$represents the relative entropy at time (t_1), while $H_n(t_2)$ signifies the relative entropy at time (t_2). The alteration in entropy can be employed to determine whether land development adheres to a more scattered (sprawled) or concentrated pattern of urban expansion. When the relative Shannon's entropy value exceeds 0.5 (the threshold), it indicates urban sprawl in the area. Conversely, if the result falls below 0.5, it suggests a densely developed built-up area. The study area has been divided into distinct zones to investigate the expansion of urban sprawl. (Bhatta *et al.*, 2010a) partitioned the research area into eight pie sections to evaluate urban sprawl. (Sudhira *et al.*, 2004b) highlighted significant factors in urban growth such as roads and city centers. They established buffer zones around these factors to quantify urban expansion (Sabet *et al.*, 2011) established a concentric circular zone around the center of the research area to evaluate its growth. In our current research, despite having access to well-defined administrative and ward boundaries in the study area, we opted not to utilize them. This decision was based on the fact that these wards experience alterations in both their geographical size and number over time, with the aim of enhancing administrative efficiency and effectiveness. In this study, we divided the research region starting from Herat Government Office, which is located in the center of Herat city. Here, we employed relative Shannon's entropy, which is not constrained by the number of divisions and remains unaffected by the manner in which we segment the study area (Bhatta *et al.*, 2010b; Patra *et al.*, 2022a). Therefore, we divide the study area into eight pie sections starting from the Herat Government Office. The study area encompasses eight primary compass directions, which include East (E), Northwest (NW), North (N), West (W), Southwest (SW), South (S), and South-east (SE). Each of these zones is further divided into a concentric circle arrangement with a radius of 3 kilometers, aiming to examine urban sprawl comprehensively across every nook and cranny of Herat City. In total, 27 vector maps of the research area have been generated and are employed to delineate 27 zones within which the raster image is extracted **Fig. 2**.

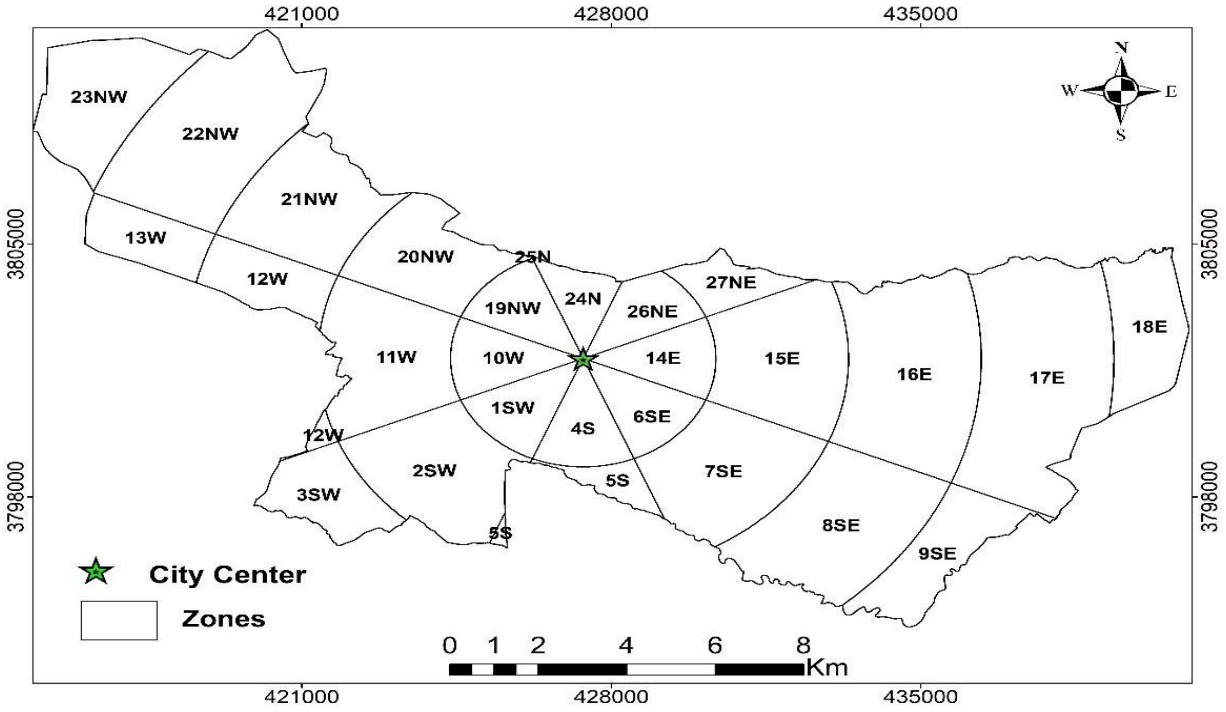

Fig. 2: Zone division of study area.

Land-use/Cover Classification

The Google Earth Engine (GEE) JavaScript API Code Editor was utilized to access information from satellite images. GEE provides access to a wide range of publicly available image data and offers an API for performing analysis and creating visualizations with this data (Sahak *et al.*, 2023). Data on surface reflectance from Landsat 7 and 8 were gathered using the

USGS Landsat surface reflectance tier 1 dataset available through Google Earth Engine. Surface reflectance was computed by utilizing data from Landsat (TM, OLI/TIRS) sensors that have undergone orthorectification and atmospheric correction. For this analysis, bands one through seven were employed, and the resulting spatial resolution was set at 30 meters. Temporal aggregation was employed in conjunction with filters for geographical boundaries, dates, and cloud cover. This process also included the computation of both the mean and median values when selecting bands of reflectance values from all available images for each specific study period. Consequently, for every study timeframe and aggregation method, a solitary image with seven bands was created. In this study, three supervised algorithms were employed: SVM, RF, and CART. In this research, 80 percent of the data were utilized for training purposes, while 20 percent were reserved for testing, for each of the algorithms. The accuracy of each algorithm was assessed. Based on the results, the RF supervised algorithm consistently provided higher classification accuracy for each study period. Therefore, the RF algorithm was chosen as the classification method. For each time interval, the study area has been categorized into four groups: Built-Up, Vegetation, Water, and Barren Land, and the outputs are demonstrated in **Fig. 3**.

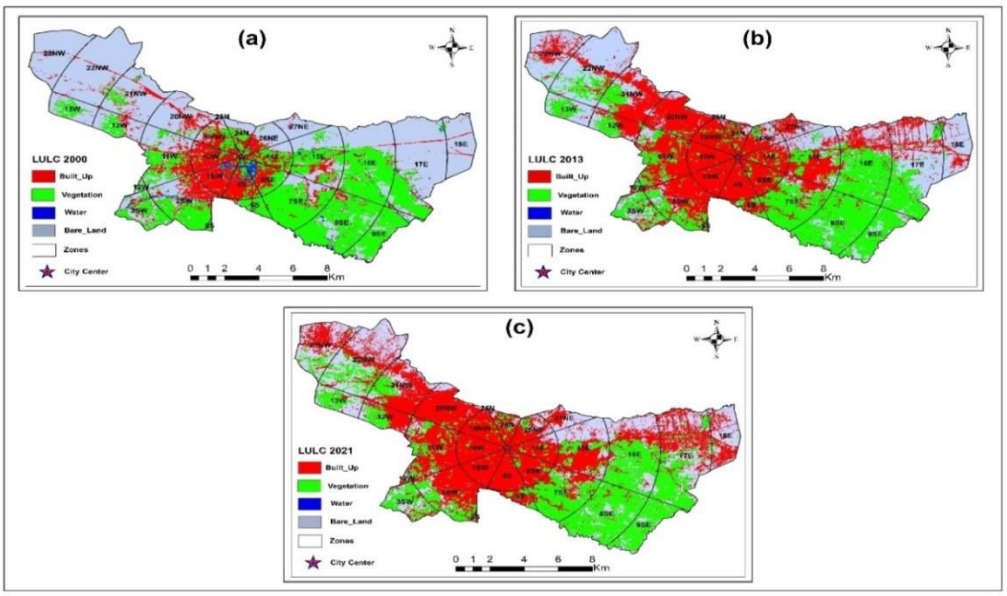

Fig. 3: Spatial dynamics of LU/LC in Herat City; (a) 2000, (b) 2013, and (c) 2021.

RESULTS AND DISCUSSION:

As stated above, in this study, three supervised machine learning algorithms were employed: SVM, RF, and CART. In this research, 20 percent of the data were utilized for testing purposes, while 80 percent were reserved for training, for each of the algorithms. The accuracy of each algorithm for every study period was assessed respectively. The outputs of the assessment are demonstrated in **Table 3**. Based on **Table 3**, the results indicate that in the year 2000, the overall accuracy for SVM, RF, and CART algorithms was 94%, 98%, and 97%, respectively, with corresponding Kappa coefficients of 0.81, 0.93, and 0.91, respectively. In 2013, the overall accuracy for SVM, RF, and CART algorithms changed to 88%, 92%, and 88%, while the Kappa coefficients for each algorithm were estimated at 0.82, 0.88, and 0.81, respectively. Consequently, in 2021, the outputs demonstrate that the overall accuracy for each algorithm is as follows: 84%, 88%, and 84%, with corresponding Kappa coefficients of 0.74, 0.81, and 0.76, respectively. Based on the overall evaluation, the RF supervised algorithm consistently provided higher classification accuracy for each study period. Therefore, the RF algorithm was chosen as the classification method. The findings indicated that various land cover tegories, including built-up areas, water bodies, vegetation, and barren land, were accurately recognized.

Accuracy assessment of LU/LC classification

Table 3: Accuracy assessment of LU/LC classification in 2000, 2013, and 2021.

Year	Built_Up		Vegetation		Water		Bare_Land		Overall Accuracy (%)	Kappa Index	Algorithm
	User's Accuracy (%)	Producer Accuracy (%)	User's Accuracy (%)	Producer Accuracy (%)	User's Accuracy (%)	Producer Accuracy (%)	User's Accuracy (%)	Producer Accuracy (%)			
2000	81	91	99	98	75	95	99	98	98	0.93	(RF)
	83	83	98	97	75	80	98	98	97	0.91	(CART)
	38	78	98	97	67	90	99	94	94	0.81	(SVM)
2013	90	89	96	95	76	91	93	93	92	0.88	(RF)
	85	84	92	94	61	50	90	90	88	0.81	(CART)
	80	86	95	94	79	92	91	88	88	0.82	(SVM)
2021	88	86	91	86	61	88	87	89	88	0.81	(RF)
	83	84	84	87	81	50	86	86	84	0.76	(CART)
	78	85	89	86	60	99	87	81	84	0.74	(SVM)

Assessment of changes in land use and land cover (LU/LC)

As previously stated, the study area in this research was divided into four distinct categories (Built-Up, Vegetation, Water, and Bare Land) utilizing the random forest supervised classification algorithm. This classification was employed to assess the changes in land use and land cover (LU/LC) for the years 2000, 2013, and 2021. The classified map results are depicted in **Fig. 3**. **Table 4** presents the summary statistics for the estimated areas and percentages of each LU/LC type, while **Table 5** provides summary statistics for the various changes in land use and land cover (LU/LC) observed over Herat city. In **Table 5**, a negative sign indicates a decrease in a particular land use/land cover (LU/LC) type, whereas a positive sign signifies an increase in that specific LU/LC type during the previous study period. Based on the data provided in **Table 4** and **Table 5**, there was a significant increase in the Built-up area from 26.41 km² in 2000 to 68.75 km² in 2013, signifying an expansion of 42.34 km², which corresponds to a growth of 22.77%. Conversely, the Vegetation, Water, and Bare land regions decreased from 59.05 km², 2.71 km², and 97.77 km² in 2000 to 50.00 km², 1.03 km², and 66.16 km² in 2013, resulting in a reduction of 9.05 km² (4.87%), 1.68 km² (0.90%), and 31.61 km² (17.00%), respectively. Furthermore, from 2013 to 2021, there was an increase in the built-up area, which expanded from 68.75 km² to 82.30 km², representing a growth of 13.55 km² (7.29%). In contrast, the Vegetation, Water, and Bare land regions decreased from 50.00 km², 1.03 km², and 66.16 km² to 43.21 km² (3.65% decrease), 0.84 km² (0.1% decrease), and 59.59 km² (3.53% decrease), respectively. Consequently, between 2000 and 2021, the built-up area exhibited substantial growth, increasing from 26.41 km² to 82.30 km², which represents a significant expansion of 55.89 km² (30.06%). Conversely, the Vegetation, Water, and Bare land regions decreased from their respective sizes of 59.05 km², 2.71 km², and 97.77 km² in 2000 to 43.21 km², 0.84 km², and 59.59 km² in 2021, resulting in a reduction of 15.83 km² (8.51%), 1.88 km² (1.01%), and 38.18 km² (20.53%), respectively. The overall evaluation demonstrates that the built-up areas have increased by 30.06%, indicating a high rate of urban development in Herat City over the course of 21 years.

Assessing the extent of overall urban growth

The UEII, defined as the average yearly expansion area relative to the total geographical unit area, demonstrates the potential for urban growth (Norouzi, 2023). The outcome of the overall UEII metric within the study area is displayed in **Table 6** and **Fig. 4.** Based on **Table 6** and **Fig. 4,** the results indicate that Herat city underwent high-speed development between 2000 and 2013, while experiencing medium speed development between 2013 and 2021. Moreover, the data reveals that between 2000 and 2013, the built-up area increased from 26.42 km² to 68.13 km². Furthermore, between 2013 and 2021, it expanded from 68.13 km² to 82.30 km².

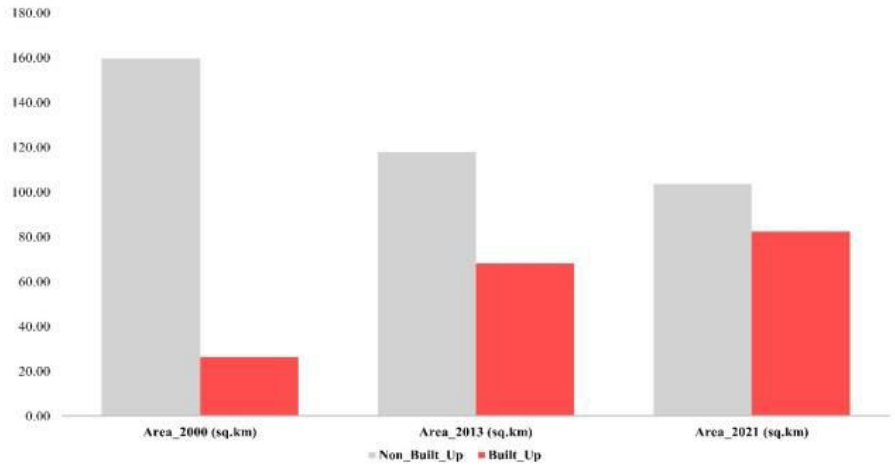

Fig. 4: The overall built-up area expansion from 2000 to 2021 in Herat city.

Table 4: Land-use/land-cover areas and percentage over Herat city in 2000, 2013, and 2021.

Type	Area_2000 (Km^2)	Area_2013 (Km^2)	Area_2021 (Km^2)	UEII (2000-2013)	UEII (2013-2021)
Non_Built_Up	159.53	117.808655	103.645	1.73	0.95

Table 5: Summary Statistics of Land-use/land cover variations over Herat city in 2000, 2013, and 2021.

Type	2000-2013 (Km^2)	2021-2013 (Km^2)	2000-2021 (Km^2)
Built_Up	41.72	14.17	55.89
Vegetation	-8.43	-7.41	-15.83
Water	-1.68	-0.19	-1.88
Bare_Land	-31.61	-6.57	-38.18

Table 6: Overall Urban Expansion Intensity Index (UEII) between 2000-2013, and 2013-2021 within Herat City.

Type	2000		2013		2021	
	Area (Km^2)	(%)	Area (Km^2)	(%)	Area (Km^2)	(%)
Built_Up	26.41	14.20	68.13	36.64	82.30	44.26
Vegetation	59.05	31.76	50.62	27.22	43.21	23.24
Water	2.71	1.46	1.03	0.55	0.84	0.45
Bare_Land	97.77	52.58	66.16	35.58	59.59	32.05

Quantification of urban expansion intensity in different cardinal direction and buffer zones

As previously mentioned, we divided the study area into eight directional sections, 27 directional zones, and five buffer ring zones with 3km radius from the Herat Government Office which is situated in the center of the Herat City. The study area comprises eight primary compass directions, 27 directional zones, which are as follows:

- East (E) (zones 14, 15, 16, 17, and 18)
- Northeast (NE) (zones 26 and 27)
- Northwest (NW) (zones 19, 20, 21, 22, and 23)
- North (N) (zones 24 and 25)
- West (W) (zones 10, 11, 12, and 13)
- Southwest (SW) (zones 1, 2, and 3)
- South (S) (zones 4 and 5)
- Southeast (SE) (zones 6, 7, 8, and 9).

This visualization aims to depict the speed and scale of urban expansion in each direction (see **Fig. 5**), and also in this study the speed and scale of urban expansion evaluated in in each 3km ring buffer zones. These buffer zones are viewed as fundamental spatial units used to describe the spatiotemporal pattern of urban development over specific distances. **Table 7** and **Fig. 6** present the summary statistics for the estimated area of urban area and urbanization intensity

index in each direction and directional zones. Based on the data presented in **Table 7** and **Fig. 6**, the findings indicate that between 2000 and 2013, the built-up area increased from 4.321 km², 4.038 km², 5.443 km², and 5.928 km² to 17.886 km², 14.219 km², 11.374 km², and 9.989 km², representing expansions of 13.57 km², 10.18 km², 5.93 km², and 4.06 km² in the NW (zones 19, 20, 21, 22, and 23), E (zones 14, 15, 16, 17, and 18), W (zones 10, 11, 12, and 13), and SW (zones 1, 2, and 3) directions and respective zones. Meanwhile, in the S (zones 4 and 5), SE (zones 6, 7, 8, and 9), N (zones 24 and 25), and NE (zones 26 and 27) directions, the built-up area changed from 2.492 km², 2.877 km², 0.514 km², and 0.798 km² to 9.984 km², 5.621 km², 1.514 km², and 3.226 km², indicating expansions of 1.81 km², 2.74 km², 1 km², and 2.43 km², respectively. Between 2013 and 2021, the data reveals that the built-up area increased from 9.984 km², 4.305 km², 5.621 km², 11.734 km², 14.219 km², 17.886 km², 1.514 km², and 3.226 km², to 10.557 km², 4.940 km², 6.996 km², 13.168 km², 18.953 km², 22.355 km², 1.968 km², and 3.377 km² indicating expansions of 0.573 km², 0.635 km², 1.375 km², 1.794 km², 4.734 km², 4.469 km²,0.454 km², and 0.151 km² in the SW (zones 1, 2, and 3), S (zones 4 and 5), SE (zones 6, 7, 8, and 9), W (zones 10, 11, 12, and 13), E (zones 14, 15, 16, 17, and 18), NW (zones 19, 20, 21, 22, and 23), N (zones 24 and 25), and NE (zones 26 and 27) directions and respective zones.

The overall assessment indicates that between 2000 and 2013, the largest expansion of the built-up area occurred in the NW (zones 19, 20, 21, 22, and 23), E (zones 14, 15, 16, 17, and 18), W (zones 10, 11, 12, and 13), and SW (zones 1, 2, and 3) directions and zones. Meanwhile, from 2013 to 2021, the greatest expansion of the built-up area was observed in the E (zones 14, 15, 16, 17, and 18) and NW (zones 19, 20, 21, 22, and 23) directions and zones. Once again, based on the data from **Table 7**, between 2000 and 2013, the highest urban expansion intensity occurred in the N (zones 24 and 25), NE (zones 26 and 27), S (zones 4 and 5), and NW (zones 19, 20, 21, 22, and 23) directions and their corresponding zones, with intensity values of 0.028%, 0.030%, 0.023%, and 0.025%, respectively. However, between 2013 and 2021, the data indicates that the maximum urban intensity was observed in the N (zones 24 and 25), NW (zones 19, 20, 21, 22, and 23), E (zones 14, 15, 16, 17, and 18), S (zones 4 and 5), and W (zones 10, 11, 12, and 13) directions and their associated zones, with intensity values of 0.016%, 0.012%, 0.011%, and 0.01%, respectively. The summary statistics for the estimated area of built-up areas and the urbanization intensity index in each buffer rings are presented in **Table 8** and **Fig. 7**.

The findings reveal that between 2000 and 2013, the built-up areas expanded from 13.254 km^2, 8.0403 km^2, 3.09 km2, 1.296 km^2, and 0.401 km^2 to 22.231 km2, 26.571 km^2, 11.003 km^2, 5.151 km^2, and 3.203 km^2, respectively. This indicates an expansion of 8.98 km^2, 18.17 km^2, 7.91 km^2, 3.85 km^2, and 2.80 km^2, with urban expansion intensities of 0.025%, 0.027%, 0.013%, 0.007%, and 0.014% in the 3km, 6km, 9km, 12km, and 15km buffer zones, respectively. Furthermore, the results indicate that between 2013 and 2021, the built-up areas increased from 22.231 km^2, 26.571 km^2, 11.003 km^2, 5.151 km^2, and 3.203 km^2 to 22.795 km^2, 31.07 km^2, 12.628 km^2, 9.50 km^2, and 6.34 km^2, respectively. This represents expansions of 1.57 km2, 4.5 km^2, 1.63 km^2, 4.35 km^2, and 3.14 km^2, with urban expansion intensities of 0.007%, 0.01%, 0.005%, 0.013%, and 0.023% in the 3km, 6km, 9km, 12km, and 15km buffer zones, respectively. The overall assessment indicates that the maximum urban expansion and urban expansion intensity occurred between 2000 and 2013 in each buffer zone, respectively. Based on data from the United Nations (UN) and the International Committee of the Red Cross (ICRC), approximately 730,000 individuals have been forced to leave their homes in Afghanistan due to conflict since 2006, leading to an average of 400 people being internally displaced every day (APPRO, 2012). The drought in 2006, along with subsequent food shortages and a harsh winter in 2007 and 2008, coupled with the global rise in the costs of essential food items in 2008, resulted in the emergence of numerous newly displaced and resettled populations (APPRO, 2012). In 2011, UNHCR estimated that there were 447,547 internally displaced persons (IDPs) in Afghanistan, with 43 percent of them being a result of conflict (APPRO, 2012). As a result, conflicts, insufficient employment opportunities, and limited living amenities in rural regions served as the primary factors driving internal migration towards major cities, ultimately contributing to the urban development in Afghanistan.

Table 7: Urban Expansion Intensity Index (UEII) in each direction and directional zone between 2000, 2013, and 2021in Herat.

Direction	Directional zone	Built-Up Area 2000 (Km^2)	Built-Up Area 2013 (Km^2)	Built-Up Area 2021 (Km^2)	UEII (2000-2013) (%)	UEII (2013-2021) (%)
SW	1	5.928	9.98	10.557	0.0173	0.004
	2					
	3					
S	4	2.492	4.30	4.940	0.0246	0.012
	5					
SE	6	2.877	5.62	6.996	0.0066	0.006
	7					
	8					
	9					
W	10	5.443	11.37	13.168	0.0205	0.01
	11					
	12					
	13					
E	14	4.038	14.22	18.953	0.0144	0.011
	15					
	16					
	17					
	18					
NW	19	4.321	17.89	22.355	0.0235	0.012
	20					
	21					
	22					
	23					
N	24	0.514	1.51	1.968	0.0281	0.016
	25					
NE	26	0.796	3.23	3.377	0.0297	0.003
	27					

Table 8: Urban Expansion Intensity Index (UEII) in each 3km buffer zone between 2000, 2013, and 2021.

Buffer Ring	Built-Up Area 2000 (Km^2)	Built-Up Area 2013 (Km^2)	Built-Up Area 2021 (Km^2)	UEII (2000-2013) (%)	UEII (2013-2021) (%)
3 Km	13.25	22.23	23.80	0.0250	0.0068
6 Km	8.40	26.57	31.07	0.0269	0.0096
9 Km	3.09	11.00	12.63	0.0131	0.0050
12 Km	1.30	5.15	9.50	0.0068	0.0135
15 Km	0.40	3.20	6.34	0.0136	0.0229

Relative Shannon's Entropy for the Urban Sprawl Analysis

Shannon's entropy quantifies the degree of spatial compactness or dispersion of a geophysical parameter within a set of n zones (Al-sharif *et al.*, 2016; Jat *et al.*, 2008a). In this study, the built-up area is regarded as a geophysical factor, and it is employed to examine urban growth (including overall expansion, expansion in each cardinal direction, and expansion in each of the 27 zones) across the entire time frame within the study area. The entropy and relative entropy values over the years in the overall study area, each cardinal direction, and across 27 distinct zones are displayed in **Table 9**, **Table 10** and **Table 11**. The relative Shannon's entropy scale ranges from 0 to 1. A value closer to 0 signifies a tightly packed or concentrated distribution of urban areas, while a value closer to 1 indicates urban sprawl in a more scattered fashion. Therefore, increased entropy corresponds to a greater extent of urban sprawl (Al-sharif *et al.*, 2016; Jat *et al.*, 2008a). The critical threshold for relative Shannon's entropy is set at 0.5. If the value is below 0.5, it signifies a con-

centrated urban area distribution, whereas a value above 0.5 indicates urban sprawl. The overall relative Shannon's entropy of Herat City is demonstrated in **Table 9**.

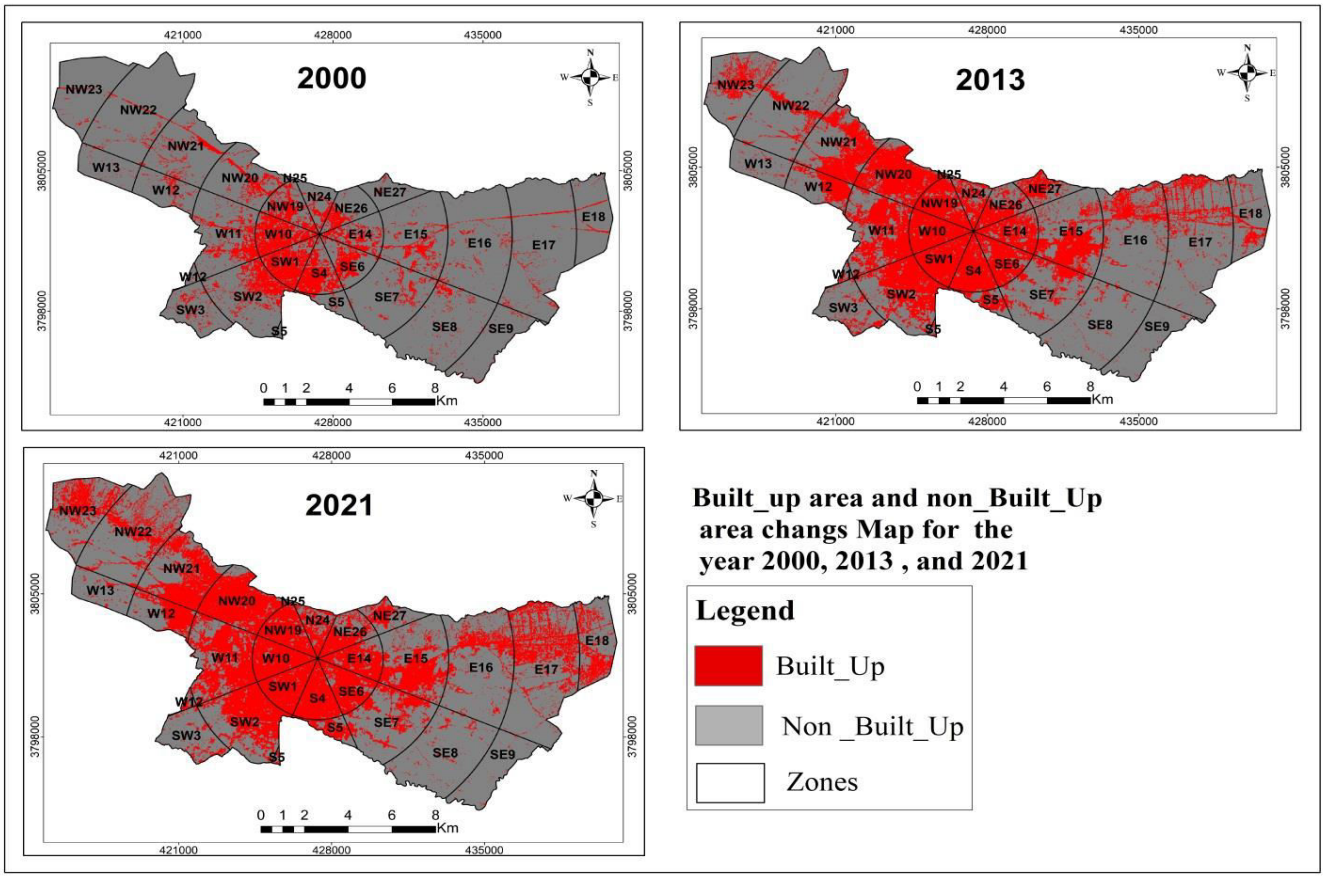

Fig. 5: Built-Up Area expansion in each direction and directional zone within Herat City; (a) 2000, (b) 2013, and (c) 2021.

According to **Table 9**, the data reveals that in 2000, the overall relative Shannon's entropy value was 0.696. In 2013, it reached 0.795, and in 2021, it reached 0.791. Therefore, the overall relative Shannon's entropy value exceeded the threshold of 0.5, indicating the expansion of Herat City in a sprawling manner throughout the study period. Furthermore, the outputs indicate that the highest relative Shannon's entropy value occurred in 2013, while the lowest value was recorded in 2000. **Table 10**, **Table 11**, and **Table 12** display the relative Shannon's entropy values for each cardinal direction and zones. Based on the data, in 2000 the highest relative Shannon's entropy values are observed in the SW directions (zones 1, 2, and 3), S direction (zones 4 and 5), and W direction (zones 10, 11, 12, and 13), as well as in the respective zones. Conversely, the lowest values are recorded in the SE directions (zones 6, 7, 8, and 9), E direction (zones 14, 15, 16, 17, and 18), and NW direction (zones 19, 20, 21, 22, and 23), along with the corresponding zones. Furthermore, in 2013, the highest relative Shannon's entropy values are found in the NE direction (zones 26 and 27), N direction (zones 24 and 25), NW direction (zones 19, 20, 21, 22, and 23), E direction (zones 14, 15, 16, 17, and 18), and W direction (zones 10, 11, 12, and 13) along with their respective zones. The lowest value is measured in the S direction (zones 4 and 5) and their corresponding zones. Moreover, in 2021, the highest relative Shannon's entropy value is estimated in the NE direction (zones 26 and 27), E direction (zones 14, 15, 16, 17, and 18), NW direction (zones 19, 20, 21, 22, and 23), N direction (zones 24 and 25), and SE directions (zones 6, 7, 8, and 9) and their corresponding zones. **Table 13** demonstrates the rate of change in urban sprawl rate between 2000, 2013, and 2021. Based on the outcomes, between 2000 and 2013 the maximum rate of change in urban sprawl is estimated in E (zones14, 15, 16, 17, and 18), NW (zones 19, 20, 21,

22, and 23), SE (zones 6, 7, 8, and 9), and NE (zones 26 and 27) directions and zones, while the minimum rate of change in urban sprawl is observed in S (zones 4 and 5), SW (zones1, 2, and 3), W (zones 10, 11, 12, and 13), and N (zones 24 and 25) directions and zones. Moreover, between 2013 and 2021, the outputs reveal that the maximum rate of change in urban sprawl is estimated in E (zones 14, 15, 16, 17, and 18), SE (zones 6, 7, 8, and 9), S (zones 4 and 5), and SE (zones 6, 7, 8, and 9) directions and zones respectively, whereas the minimum values are estimated in NW (zones19, 20, 21, 22, and 23), and W (zones 10, 11, 12, and 13), and SW (zones 1, 2, and 3) directions and zones. Furthermore, between 2000 and 2021 the maximum rate of change in urban sprawl is estimated in S (zones 4 and 5), W (zones 10, 11, 12, and 13), and SW (zones 1, 2, and 3) directions and zones, while the minimum values are measured in E (zones 14, 15, 16, 17, and 18), NW (zones 19, 20, 21, 22, and 23), NE (zones 26 and 27), and SW (zones 1, 2, and 3) directions and zones.

Table 14 indicates the statistics of the relative Shannon's entropy within each of the five buffer rings with a 3km radius from the Herat Government Office. Based on the outputs in **Table 14**, in 2000, the maximum relative Shannon's entropy values are measured in the 3km, 6km, and 9km buffer rings, respectively, while the minimum values are recorded in the 12km and 15km buffer zones.

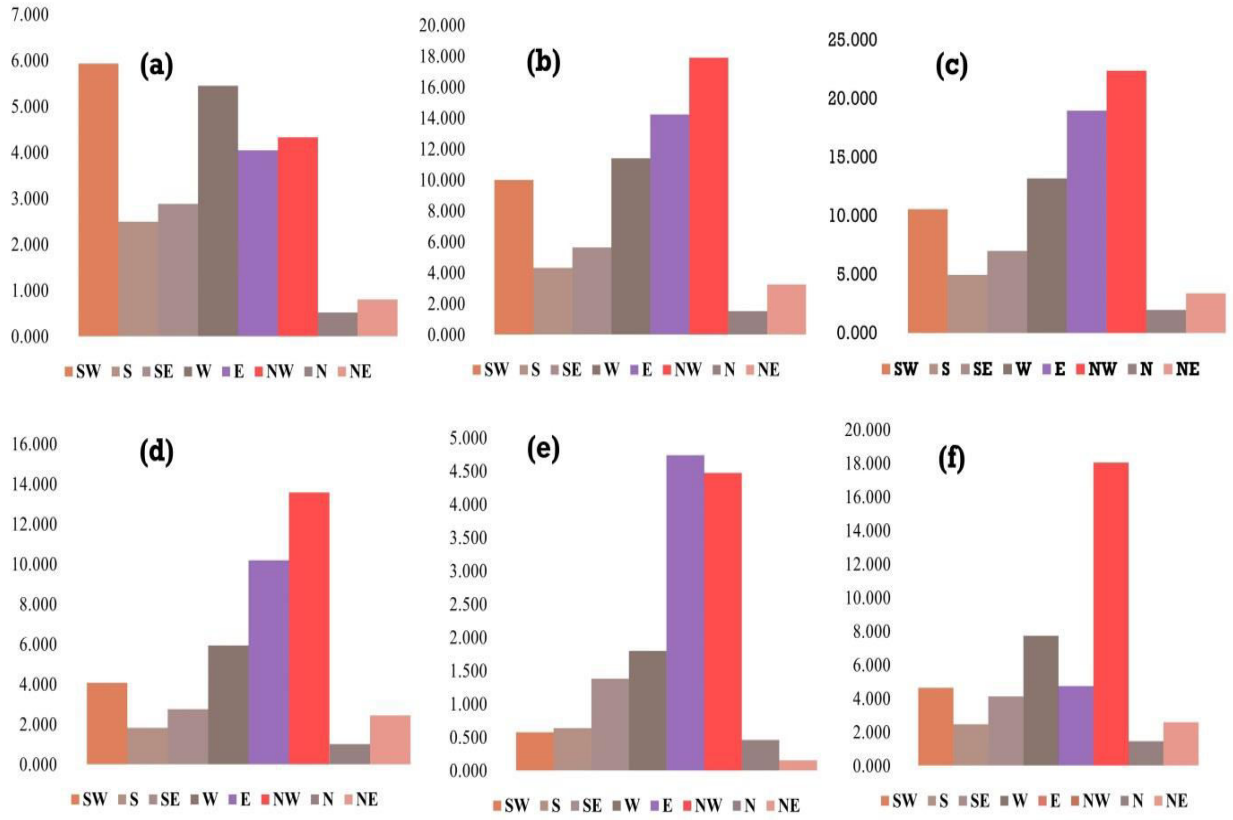

Fig. 6: Statistics of Built-Up area expansion and changes in each direction and directional zone; (a), (b), and (c) Built-Up area expansion, and (d), (e), and (f) Built-Up area changes.

Table 9: Overall relative Shannon's entropy of Herat city (2000 - 2021).

Year	Relative Shannon Entropy
2000	0.696
2013	0.795
2021	0.791

Table 10: Summary statistics of Shannon's Entropy values in 2000 for each direction and directional zone.

Direction	Directional zone	Built-Up Area 2000 (Km^2)	Total Area in Each Direction (Km^2)	Shannon's Entropy Algorithm		
				Absolute	Relative	Change rate (2000-2013)
SW	1	5.928	18.343	0.365	0.111	-0.012
	2					
	3					
S	4	2.492	5.414	0.357	0.108	-0.038
	5					
SE	6	2.877	32.681	0.214	0.065	0.028
	7					
	8					
	9					
W	10	5.443	22.169	0.345	0.105	-0.001
	11					
	12					
	13					
E	14	4.038	54.636	0.193	0.058	0.048
	15					
	16					
	17					
	18					
NW	19	4.321	44.184	0.227	0.069	0.042
	20					
	21					
	22					
	23					
N	24	0.514	2.480	0.326	0.099	0.006
	25					
NE	26	0.796	6.029	0.267	0.081	0.025
	27					

Table 11: Summary statistics of Shannon's Entropy values in 2013 for each direction and directional zone.

Direction	Directional zone	Built-Up Area 2013 (Km^2)	Total Area in Each Direction (Km^2)	Shannon's Entropy Algorithm		
				Absolute	Relative	Change rate (2013-2021)
SW	1	9.984	18.343	0.325	0.098	-0.0104
	2					
	3					
S	4	4.305	5.414	0.233	0.071	0.0041
	5					
SE	6	5.621	32.681	0.306	0.093	0.0095
	7					
	8					
	9					
W	10	11.374	22.169	0.343	0.104	-0.0082
	11					
	12					
	13					
E	14	14.219	54.636	0.351	0.107	0.0049
	15					
	16					
	17					
	18					
NW	19	17.886	44.184	0.366	0.111	-0.0060
	20					
	21					
	22					
	23					
N	24	1.514	2.480	0.345	0.105	0.0019
	25					
NE	26	3.226	6.029	0.349	0.106	0.0005
	27					

In 2013, the maximum relative Shannon's entropy values are estimated in the 6km, 9km, and 15km buffer zones, whereas the minimum values are measured in the 3km and 12km buffer rings. Moreover, in 2021, the maximum relative Shannon's entropy values are measured in the 15km, 9km, 6km, 12km buffer zones.

Table 12: Summary statistics of Shannon's Entropy values in 2021 for each direction and directional zone.

Direction	Directional zone	Built-Up Area 2021 (Km^2)	Total Area in Each Direction (Km^2)	Shannon's Entropy Algorithm		
				Absolute	Relative	Change rate (2000-2021)
SW	1	10.557	18.343	0.290	0.088	0.023
	2					
	3					
S	4	4.940	5.414	0.246	0.075	0.034
	5					
SE	6	6.996	32.681	0.338	0.102	-0.038
	7					
	8					
	9					
W	10	13.168	22.169	0.316	0.096	0.009
	11					
	12					
	13					
E	14	18.953	54.636	0.368	0.112	-0.053
	15					
	16					
	17					
	18					
NW	19	22.355	44.184	0.347	0.105	-0.036
	20					
	21					
	22					
	23					
N	24	1.968	2.480	0.351	0.107	-0.008
	25					
NE	26	3.377	6.029	0.350	0.106	-0.025
	27					

Table 13: Summary statistics rate of change in urban sprawl in (2000 - 2021) for each direction and directional zone in Herat city.

Direction	Directional zone	Rate of change in urban sprawl		
		Change rate (2000-2013)	Change rate (2013-2021)	Change rate (2000-2021)
SW	1	-0.012	-0.0104	0.023
	2			
	3			
S	4	-0.038	0.0041	0.034
	5			
SE	6	0.028	0.0095	-0.038
	7			
	8			
	9			
W	10	-0.001	-0.0082	0.009
	11			
	12			
	13			
E	14	0.048	0.0049	-0.053
	15			
	16			
	17			
	18			
NW	19	0.042	-0.0060	-0.036
	20			
	21			
	22			
	23			
N	24	0.006	0.0019	-0.008
	25			
NE	26	0.025	0.0005	-0.025
	27			

Table 14: Summary statistics of Shannon's Entropy values from 2000 to 2021 within each 3km buffer ring over Herat City.

Year	Buffer Ring (3Km)	Absolute	Relative	Change rate in urban sprawl (2000 - 2013)
2000	3Km	0.349	0.2168	-0.0981
	6Km	0.293	0.1822	0.0300
	9Km	0.179	0.1111	0.1014
	12Km	0.103	0.0642	0.0930
	15Km	0.096	0.0599	0.1377
				Change rate in urban sprawl (2013 - 2021)
2013	3Km	0.191	0.1187	-0.0143
	6Km	0.342	0.2123	0.0076
	9Km	0.342	0.2124	0.0160
	12Km	0.253	0.1573	0.0592
	15Km	0.318	0.1976	0.0309
				Change rate in urban sprawl (2000 - 2021)
2021	3Km	0.168	0.1044	-0.1124
	6Km	0.354	0.2199	0.0377
	9Km	0.368	0.2284	0.1173
	12Km	0.348	0.2165	0.1523
	15Km	0.368	0.2285	0.1686

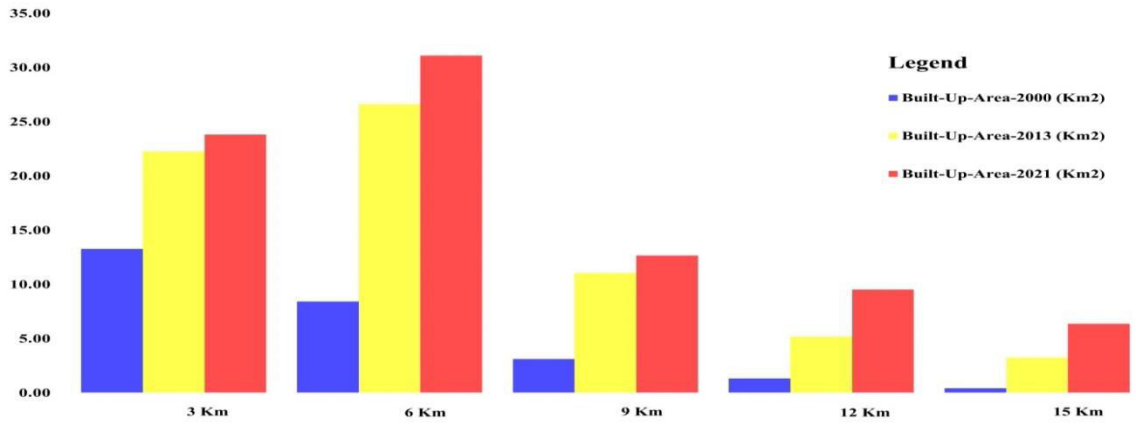

Fig. 7: Built-up area changes in each buffer ring (1, 2, 3, 4, and 5).

While the minimum value is recorded in the 3km buffer zone. Again, according to the results in **Table 14,** the most significant increase in the change of urban sprawl rate between 2000 and 2013 is observed in the 15km and 9km buffer zones, with urban sprawl rates of 0.1444 and 0.1, respectively. Conversely, the lowest urban sprawl rate is recorded in the 3km buffer zone, indicating a decrease of -0.118 between 2000 and 2013. Furthermore, between 2013 and 2021, the maximum change in urban sprawl rate is estimated in the 12km and 15km buffer zones, with urban sprawl rates of 0.059 and 0.031, respectively, while the minimum change in urban sprawl rate is recorded in the 3km and 6km buffer zones, with a change in urban sprawl rate of -0.014 and 0.008, respectively.

Furthermore, the overall assessment of the change in urban sprawl rate between 2000 and 2021 indicates that the highest change in urban sprawl rate is estimated in the 15km, 12km, and 9km buffer zones, with change in urban sprawl rates of 0.169, 0.152, and 0.117, respectively, while the minimum change in urban sprawl rate is estimated in the 3km and 6km buffer zones, with a change in urban sprawl rate of -0.112 and 0.038, respectively. Consequently, as stated above internal migration to major cities in Afghanistan was predominantly motivated by conflicts, a lack of

employment opportunities, and limited access to essential amenities in rural areas. This migration has played a significant role in the change in urban sprawl rates over the study period in Herat City.

CONCLUSION:

To attain sustainable development and foster a policy of continuous urban growth, uncontrolled urban development stands as a possible risk. The current study aims to evaluate the trends and progression of urban expansion within Herat City. The objective is to provide urban planners with insights to enhance and implement more effective and sustainable urban development strategies. Temporal satellite imagery was employed in urban growth modeling to classify and analyze changes in land use and land cover characteristics over the study period. In this research, three different machine learning algorithms are used to classify the study area:

Support Vector Machine (SVM), Smile Random Forest (SRF), and Classification and Regression Trees (CART). The accuracy of each algorithm was evaluated for different study periods. After evaluating their performance, the Random Forest (RF) algorithm was found to have the highest accuracy and was chosen as the classification method. The classification of the study area was carried out using the Google Earth Engine cloud platform, and thematic layers were created within a Geographic Information System (GIS) environment. The study area was divided into eight directional sections, 27 directional zones, and five ring buffer zones with 3km radius from the center of the city. The Urban Expansion Intensity Index was used to measure the urban expansion speed from 2000 to 2021. From 2000 to 2013, Herat City saw an overall high-speed urban expansion; while from 2013 to 2021, the city's urban expansion occurred at a medium speed. This suggests that during this period, there was rapid development, significant population growth, and an increase in infrastructure and construction activities in the city. The Relative Shannon's entropy statistical algorithm was used to analyze the pace of transformation in urban sprawl, compactness, and the dispersed pattern of the built-up environment in various cardinal directions, directional zones, buffer rings, and across the entire research area. The overall Relative Shannon's entropy values changed from 0.696 to 0.0.795 and 0.791 from 2000, 2013 and 2021 within Herat City respectively. These values suggest that Herat City experienced a trend of increasingly scattered urban expansion throughout the entire study period. In general, the analysis shows that Herat City experienced a transition from a less dispersed urban sprawl pattern in 2000 to a more dispersed by 2013, and this trend continued to 2021. The practical study of built-up density patterns within urban areas, as outlined in this paper, provides a new perspective on how policy adjustments can impact spatial arrangements. This analysis has the capacity to assist urban planners and policymakers in assessing the effectiveness of policies aimed at urban consolidation or developing compact cities.

ACKNOWLEDGEMENT:

I would like to thank our colleagues for their assistance and guidance in helping us successfully complete this work.

CONFLICTS OF INTEREST:

The authors declare that there is no conflict of interest to publish it.

REFERENCES:

1) Abubakr A. A. Alsharif, Biswajeet Pradhan, Shattri Mansor, H. Z. M. S. (2015). Urban Expansion Assessment by Using Remotely Sensed Data and the Relative. *Theoretical and Empirical Researches in Urban Manag.*, **10**(1).
2) Aguilera, F., Valenzuela, L. M., & Botequilha-Leitão, A. (2011). Landscape metrics in the analysis of urban land use patterns: A case study in a Spanish metropolitan area. *Landscape and Urban Planning*, **99**(3-4), 226-238. https://doi.org/10.1016/j.landurbplan.2010.10.004
3) Ali Mahaqi, Moheghy, M. A., Moheghi, M. M., & Zandvakili, Z. (2020). Environmental Hydrogeochemistry Characteristics, Controlling Factors and Groundwater Quality Assessment in Herat City, West Afghanistan. *Water Resources*, **47**(2), 325-335. https://doi.org/10.1134/S0097807820020104
4) Alom MJ. (2024). Blueprints for progress: unveiling the pillars of urban evolution in contemporary American metropolises, *Asian J. Soc. Sci. Leg. Stud.*, **6**(3), 70-76.

5) Al-sharif, A. A. A., Pradhan, B., Shafri, M. (2016). Quantitative analysis of urban sprawl in Tripoli using Pearson's Chi-Square statistics and urban expansion intensity index Quantitative analysis of urban sprawl in Tripoli using Pearson's Chi-Square statistics and urban expansion intensity index. https://doi.org/10.1088/1755-1315/20/1/012006
6) Antalyn, B., & Weerasinghe, V. P. A. (2020). Assessment of Urban Sprawl and Its Impacts on Rural Landmasses of Colombo District: A Study Based on Remote Sensing and GIS Techniques. *Asia-Pacific J. of Rur. Devel.*, **30**(1-2), 139-154.
7) APPRO. (2012). Migration and {Urban} {Development} in {Kabul}: {Classification} or {Accommodation}? {Newcomers} and {Host} {Communities} in {Districts} 5, 7, and 13 in {Kabul}, {Afghanistan}. October, 30.
8) Bhatta, B. (2009). Analysis of urban growth pattern using remote sensing and GIS: A case study of Kolkata, India. *Inter. J. of Remote Sensing*, **30**(18), 4733-4746.
9) Bhatta, B., Saraswati, S., & Bandyopadhyay, D. (2010a). Urban sprawl measurement from remote sensing data. **30**, 731-740. https://doi.org/10.1016/j.apgeog.2010.02.002
10) Bhatta, B., Saraswati, S., & Bandyopadhyay, D. (2010b). Urban sprawl measurement from remote sensing data. *Appl. Geo.*, **30**(4), 731-740.
11) Boori, M. S., Netzband, M., & Voženílek, V. (2015). Monitoring and modeling of urban sprawl through remote sensing and GIS in Kuala Lumpur, Malaysia. *Ecological Processes*, **4**(1), 1-10. https://doi.org/10.1186/s13717-015-0040-2
12) Jat, M. K., Garg, P. K., & Khare, D. (2008a). Modelling of urban growth using spatial analysis techniques: A case study of Ajmer city (India). *Inter J. of Remote Sensing*, **29**(2), 543-567.
13) Jat, M. K., Garg, P. K., & Khare, D. (2008b). Monitoring and modelling of urban sprawl using remote sensing and GIS techniques. *Inter. J. of Appl. Earth Obser.and Geoinform.*, **10**(1), 26-43.
14) Keita, M. A., Ruan, R., & An, R. (2021). Spatio-temporal Change of Urban Sprawl Patterns in Bamako District in Mali Based on Time Series Analysis. *Urban Science*, **5**(1). https://doi.org/10.3390/urbansci5010004
15) Kristy, G. (2018a). The impact of urban sprawl on cultural heritage in Herat, Afghanistan: A GIS analysis. *Digital Applications in Archaeology and Cultural Heritage*, **11**(November), 1-8.
16) Kristy, G. (2018b). The impact of urban sprawl on cultural heritage in Herat, Afghanistan: A GIS analysis. *Digital Applications in Archaeology and Cultural Heritage*, **11**(November), 1-8.
17) Liu, L., & Meng, L. (2020). Patterns of Urban Sprawl from a Global Perspective. *J. of Urban Planning and Development*, **146**(2), 1-9.
18) Manesha, E. P. P., Jayasinghe, A., & Kalpana, H. N. (2021). Measuring urban sprawl of small and medium towns using GIS and remote sensing techniques: A case study of Sri Lanka. *Egyptian Journal of Remote Sensing and Space Science*, **24**(3P2), 1051-1060. https://doi.org/10.1016/j.ejrs.2021.11.001
19) Milad, M., Ho, S., & Firuz, M. (2017). Measuring and Mapping Urban Growth Patterns Using Remote Sensing and GIS Techniques. **3**, 55-69.
20) Mosammam, H. M., Nia, J. T., & Kazemi, M. (2017). Monitoring land use change and measuring urban sprawl based on its spatial forms: The case of Qom city. *Egyptian J. of Remote Sensing and Space Science*, **20**(1), 10-116.
21) Nasery, S., Matci, D. K., & Avdan, U. (2021a). GIS-based wind farm suitability assessment using fuzzy AHP multi-criteria approach: the case of Herat, Afghanistan. *Arab. J. of Geosci.*, **14** (12). https://doi.org/10.1007/s12517-021-07478-5
22) Nasery, S., Matci, D. K., & Avdan, U. (2021b). GIS-based wind farm suitability assessment using fuzzy AHP multi-criteria approach: the case of Herat, Afghanistan. *Arab. J. of Geosci.*, **14** (12). https://doi.org/10.1007/s12517-021-07478-5
23) Nejadi, A., Salehi, E., & Jafari, M. (2011). Investigating urban sprawl metrics and dynamics using RS and GIS - Case study: Gilan province, IRAN. *2011 Joint Urban Remote Sensing Event, JURSE 2011 - Proceedings*, 441-444.
24) Norouzi, Y. (2023). Measuring Land Use Changes and Quantifying Urban Expansion Using Remote Sensing and Gis Techniques - a Case Study of Qom. *ISPRS Annals of the Photogrammetry, Remote Sensing and Spatial Information Sciences*, **10**(4/W1-2022), 609-615.

25) Páez, A., & Scott, D. M. (2004). Spatial statistics for urban analysis: A review of techniques with examples. *Geo Journal*, **61**(1), 53-67.
26) Patra, P. K., Behera, D., & Goswami, S. (2022a). Relative Shannon's Entropy Approach for Quantifying Urban Growth Using Remote Sensing and GIS: A Case Study of Cuttack City, Odisha, India. *J. of the Ind. Soc. of Rem. Sen.*, **50**(4), 747 -762. https://doi.org/10.1007/s12524-022-01493-z
27) Patra, P. K., Behera, D., & Goswami, S. (2022b). Relative Shannon's Entropy Approach for Quantifying Urban Growth Using Remote Sensing and GIS: A Case Study of Cuttack City, Odisha, India. *J. of the Indian Society of Remote Sensing*, **50**(4), 747-762.
28) Rahman, A., Aggarwal, S. P., & Fazal, S. (2011). Monitoring Urban Sprawl Using Remote Sensing and GIS Techniques of a Fast Growing Urban Centre, India. *IEEE J. of Sel. Top. in Appl. Earth Obs. and Remote Sensing*, **4**(1), 56-64. https://doi.org/10.1109/JSTARS.2010.2084072
29) Ramachandra, T. V., Bharath, H. A., & Sowmyashree, M. V. (2013). Analysis of spatial patterns of urbanisation using geoinformatics and spatial metrics. *Theoretical and Empirical Researches in Urban Management*, **8**(4), 5-24.
30) Sabet Sarvestani, M., Ibrahim, A. L., & Kanaroglou, P. (2011). Three decades of urban growth in the city of Shiraz, Iran: A remote sensing and geographic information systems application. *Cities*, **28**(4), 320-329.
31) Sahak, A. S., Karsli, F., & Ahmadi, K. (2023). Seasonal monitoring of urban heat island based on the relationship between land surface temperature and land use/cover: a case study of Kabul City, Afghanistan. *Ear. Sci. Inf.*, **16**(1), 845-861. https://doi.org/10.1007/s12145-022-00918-0
32) Sudhira, H. S., & Ramachandra, T. V. (2007). Characterising urban sprawl from remote sensing data and using landscape metrics. *Proceedings of 10th International Conference on Computers in Urban Planning and Urban Management, CUPUM 2007*, 1-12.
33) Sudhira, H. S., Ramachandra, T. V., & Jagadish, K. S. (2004). Urban sprawl: Metrics, dynamics and modelling using GIS. *Inter J. of Applied Earth Observation and Geoinformation*, **5**(1), 29-39. https://doi.org/10.1016/j.jag.2003.08.002
34) Sridhar, M. B., Sathyanathan, R., & Sudalaimathu, K. (2020). Urban Sprawl Analysis Using Remote Sensing Data and Its Impact on Surface Water Bodies: Case Study of Surat, India. *IOP Conf. Ser.: Mat. Sci. and Eng.*, **912**(6).
35) Taubenböck, H., Wegmann, M., & Dech, S. (2009). Urbanization in India - Spatiotemporal analysis using remote sensing data. *Comp., Env. and Urb. Sys.*, **33**(3), 179-188.
36) Thomas, R. W. (1981). Information statistics in geography. *Information Statistics in Geography.*
37) UN-Habitat, (2015). State of Afghan Cities 2015.
38) Urban development threatens the old city of *Herat* | UNAMA. (n.d.).
39) Verbeek, T., Boussauw, K., and Pisman, A. (2014). Presence and trends of linear sprawl: Explaining ribbon development in the north of Belgium. *Lands. and Urb. Plan.*, **128**, 48-59.
40) Verma, S., Chatterjee, A., & Mandal, N. R. (2017). Analysing urban sprawl and shifting of urban growth centre of bengaluru city, India using shannon's entropy method. *J. of Settlements and Spatial Planning*, **8**(2), 89-98. https://doi.org/10.24193/JSSP.2017.2.02
41) Wei, Y. D., & Ewing, R. (2018). Urban expansion, sprawl and inequality. *Landscape and Urban Planning*, **177**(May), 259-265.
42) Yang, J. (2018). Information Theoretic Approaches in Economics. *J. of Economic Surveys*, **32**(3), 940-960. https://doi.org/10.1111/joes.12226
43) Yeh, A. G. O., & Li, X. (2001). Measurement and monitoring of urban sprawl in a rapidly growing region using entropy. *Photogrammetric Engineering and Remote Sensing*, **67**(1), 83-90.

Citation: Sahak AS, Karsli F, Ahmadi K, Saraj MA, and Sahak AT. (2024). Geospatial assessment of urban sprawl: a case study of Herat city, Afghanistan. *Aust. J. Eng. Innov. Technol.*, **6**(3), 51-69. https://doi.org/10.34104/ajeit.024.051069